Pure Appl. Chem., Vol. 85, No. 9, pp. 1803–1811, 2013.
http://dx.doi.org/10.1351/PAC-CON-12-11-08

Sialyl*exo*enitols as precursors for new analogues of sialidase inhibitors*

Barbara Richichi[1], Carlotta Lunghi[1], Athanasios Papakyriakou[2], Oscar Francesconi[1], and Cristina Nativi[1,3,‡]

[1]Dipartimento di Chimica "Ugo Schiff", Universita' degli Studi di Firenze, via della Lastruccia, 13 50019 Sesto Florentino (FI), Italy; [2]Chemical Biology and Designed Molecules Laboratory, NCSR "Demokritos", 15310 Ag. Paraskevi, Athens, Greece; [3]CNR, Istituto di Metodologie Chimiche IMC, Area di Ricerca di Roma 1, via Salaria Km 29, 300-00015 Monterotondo, Roma, Italy

Abstract: Sialic acids are involved in a plethora of important biological events; among these the most known certainly is the binding of *N*-acetylneuraminic acid (Neu5Ac) with influenza virus sialidase. Considering Neu5Ac as the template that led to the structure-based development of the two potent antiviral agents zanamivir and oseltamivir, we developed the synthesis of the sialyl*exo*enitol, a new class of sialyl derivative that was used as precursor in powerful hetero-Diels–Alder reactions to form the corresponding spiroketals. Docking calculations employing the crystallographic structure of influenza virus sialidase indicate that these scaffolds could probably interact with most of the active site residues that stabilize Neu5Ac. In addition, their reduced polar nature with respect to Neu5Ac derivatives might provide inhibitors with increased bioavailability.

Keywords: Diels–Alder reactions; *exo*enitols; sialic derivatives; sialidase inhibitors; spiro ketals.

INTRODUCTION

Sialic acids are closely related carboxylated sugars widespread in mammalian glycoproteins and glycolipids. They are typically found at the outermost end of glycan chains of all kind of cells and are involved in a variety of physiochemical and pathological processes [1]. This class of sugars has structural and modulatory roles and serves as components of binding site for various pathogens and toxins; in addition, another important function they play is decorating microbial pathogens allowing them to evade host immunity [2].

Although sialic acids are the targets for binding by a large number of pathogenic organisms, probably their best known role is in binding of influenza viruses to airway epithelium.

Influenza virus is subdivided into three serologically distinct types: A, B, and C, all of which recognize sialic acid and its derivatives as their functional receptors. Sialidase is the influenza virus surface enzyme recognizing the sialic acid *N*-acetylneuraminic acid (Neu5Ac) moiety, which is typically associated as α-linked terminal saccharidic unit of mammalian glycoconjugates [3].

Pure Appl. Chem.* **85, 1759–1900 (2013). A collection of invited papers based on presentations at the 26th International Carbohydrate Symposium (ICS 2012), Madrid, Spain, 22–27 July 2012.
‡Corresponding author: E-mail: cristina.nativi@unifi.it

The essential roles played by sialidase in assisting the movement of virus particles through the upper respiratory tract as well as in the release of virions from infected cells fueled extensive research in sialidase structural elucidation. Structural and functional information have indeed provided great opportunities for rational structure-based discovery of anti-influenza agents [4].

At present, the two most popular structure-based inhibitors of sialidase: zanamivir **1** and oseltamivir **2** (Fig. 1) have been obtained after the determination of the X-ray crystal structure of influenza virus sialidase [5].

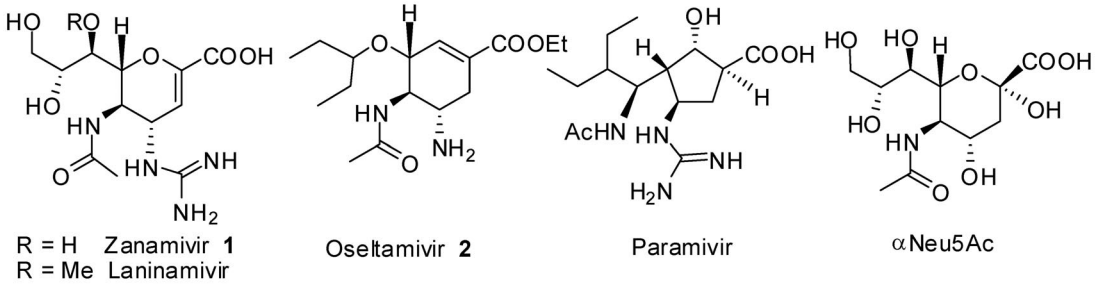

Fig. 1 Structure of zanamivir **1**, laninamivir, oseltamivir **2**, paramivir, and Neu5Ac.

Zanamivir is a drug derived from the native sialic acid Neu5Ac with slight additional functionalization. This is likely the reason why after eight years of clinical experience no unknown side-effects have been registered and no evidence exists to suggest otherwise. Conversely, in the case of oseltamivir, which is more largely used to treat influenza virus, viable resistant virus mutant has been developed [6] reducing significantly the drug efficacy. This evidence may suggest that maintaining a strong resemblance to the natural substrate Neu5Ac, the risk of the development of drug-resistant mutants might be reduced.

Hence, taking into account the almost annual risk of pandemic infections, the development of a new generation of anti-influenza drugs remains a target of high priority. However, apart from the above-mentioned zanamivir and oseltamivir, at present a very limited number of agents can be used to fight against human influenza virus infections. Quite recently, the inhibitors laninamivir and paramivir (Fig. 1) have been approved in some Asian countries [7]. Laninamivir maintains the main structural features of the potent inhibitor **1** (see Fig. 1) while paramivir is a cross-mimetic of inhibitors **1** and **2**. In the search for new sialidase-inhibitor anti-influenza drugs, sialic acid-based derivatives characterized by the replacement of the glycerol side-chain have been reported [8]. Similarly, uronic acid-based mimetics of Neu5Ac2en, in which the aglycon on the uronic acid scaffold replaces the glycerol side-chain of Neu5Ac2en (Fig. 2) have been developed [9]. Among these, compound **3**, which can be seen as a cross-mimetic of Neu5Ac2en (see Fig. 2) and oseltamivir **2** (see Fig. 1), showed an inhibition of influenza A virus sialidase in the micromolar range.

In order to allow unsaturated *O*-glucuronides-based inhibitors like **3** to adopt in solution a more favorable Neu5Ac2en-like conformation, a range of functionalities at the anomeric position of the unsaturated uronic acid scaffold have been investigated [9]. The inhibitor **4** was thus prepared in which a phosphonate group replaces the sialic acid glycerol side-chain.

Novel sialic acid-based derivatives **5** and **6** have been designed and synthesized which are able to selectively inhibit group-1 sialidase activity by locking the open and flexible 150-loop [10]. These derivatives maintain the zanamivir core structure as well as the sialic acid glycerol side-chain while the C-4 guanidino moiety has been replaced by a hydroxyl group and a hydrophobic residue at C-3 position has been incorporated. These attractive micromolar inhibitors are also effective against influenza

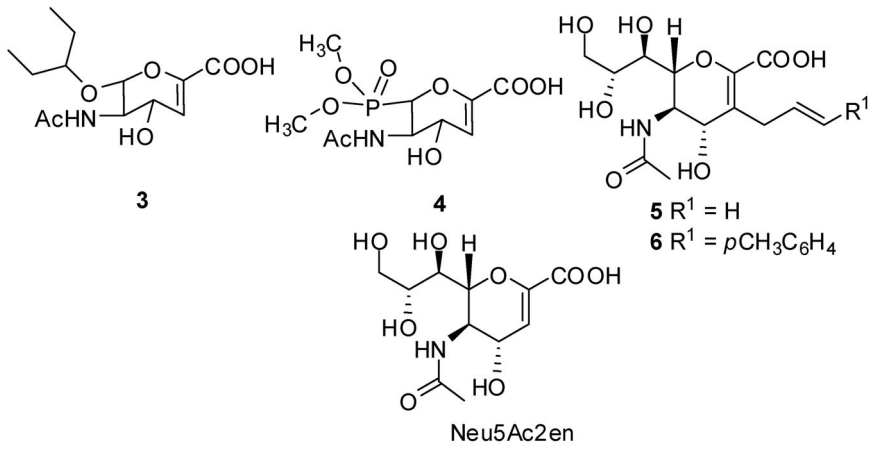

Fig. 2 Structure of compounds **3**–**6** and of Neu5Ac2en.

virus clinical isolated which contain mutations in the sialidase glycoprotein that produce resistance or reduced sensitivity to the commonly used anti-influenza drugs, oseltamivir or zanamivir [10].

In this context, we report on the synthesis of a new class of *exo*enitols [11] obtained from Neu5Ac and on their use as electron-rich dienophiles in chemo-, regio- and stereoselective hetero-Diels–Alder reactions with α,α'-dioxothiones as electron-poor dienes, to form diasteromerically pure βNeu5Ac derivatives structurally attractive for the development of new inhibitors of sialidase.

RESULT AND DISCUSSION

Synthesis of sialyl*exo*enitol

Manipulation of Neu5Ac is often frustrating because the reactivity of sialic acids is peculiar and many of the reactions successfully performed on saccharides cannot be employed when Neu5Ac is the starting material. With the aim to obtain the C-1-*exo*enitol of Neu5Ac, a new class of sialyl derivative, the commercially available Neu5Ac methyl ester **7** was protected at the primary hydroxyl group and at C-4 hydroxyl group as *tert*-butyldiphenylsilyl ether by treatment with *tert*-butyldiphenylsilyl chloride, imidazole, and a catalytic amount of *N*,*N*'-dimethylaminopyridine (DMAP) in dimethyl formamide (DMF) as solvent (rt, 20 h). The silylether **8**, formed in 73 % yield, was then transformed into the corresponding acetonide **9** by reaction with 2,2'-dimethoxypropane and camphorsulfonic acid. Reduction of the methylester residue of **9**, presenting a free hydroxyl on Cα, was successfully accomplished reacting **9** with sodium borohydride; the 1,2-diol so formed (**10**) was then oxidized to the lactone **11** (14 %, calculated over three steps) (Scheme 1).

The lactone **11** was treated with acetic acid and water (AcOH/H_2O, 4/1) for 3 h at 60 °C to remove the acetonide and to form the diol **12**, which, in turn, was reacted with Tebbe reagent in pyridine to form the *exo*enitol **13** (23 %). Clearly, the disappointing low yields obtained for the synthesis of derivatives **11** and **13** represented the limiting steps for an efficient applicability of this synthesis, so we tried to improve our synthetic strategy by reducing the number of steps and the steric hindrance of the protecting groups, which could negatively affect the reactivity of the ester **9** and the lactone **12**. Therefore, the *tert*-butyldimethylsilyl ether was chosen as new protecting group. The methyl ester **7** was thus reacted at room temperature with *tert*-butyldimethylsilyl triflate (TBDMSOTf) and pyridine, in dichloromethane as solvent, to afford the tris silyl derivative **14** in 81 % yield (Scheme 2). The replacement of the *tert*-butyldiphenylsilyl group with the less bulky *tert*-butyldimethylsilyl residue allowed the protection of the primary hydroxyl group as well as of two over the three secondary hydroxyls of the

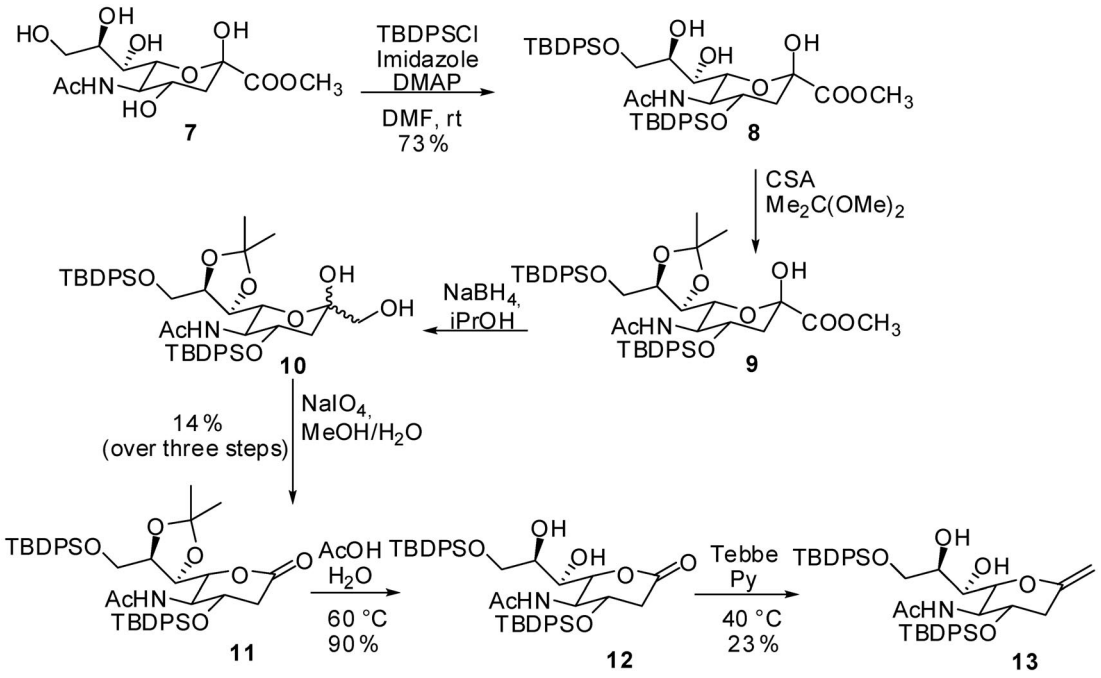

Scheme 1 Synthesis of the *exo*enitol **13**.

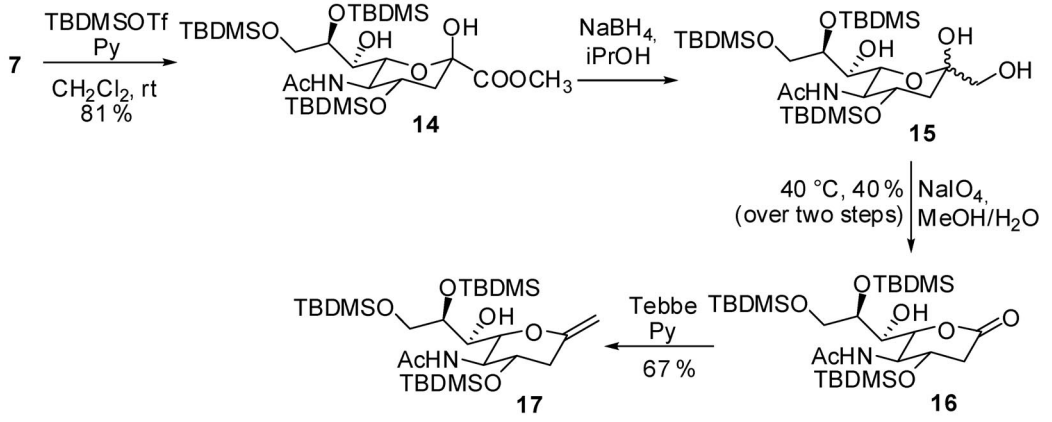

Scheme 2 Synthesis of the *exo*enitol **17**.

methyl ester **7**, thus allowing the direct reduction of **14** into **15** by treatment with sodium borohydride in *iso*-propanol. The subsequent oxidation of **15** to the lactone **16** was realized with sodium periodate in methanol/water as solvent (40 °C, 40 % yield calculated over two steps) (Scheme 2). The desired *exo*enitol **17** was finally obtained by reaction of **16** with Tebbe reagent in pyridine [12]. Compound **17** was isolated in 67 % yield as single diasteroisomer.

Synthesis of heterodienes

The heterodienes selected to react with the dienophile **17** were obtained treating the commercially available β-ketoesters **18–20** with phthalimidosolfenyl chloride (PhtNSCl) **21** and pyridine under reported conditions [13] (Scheme 3).

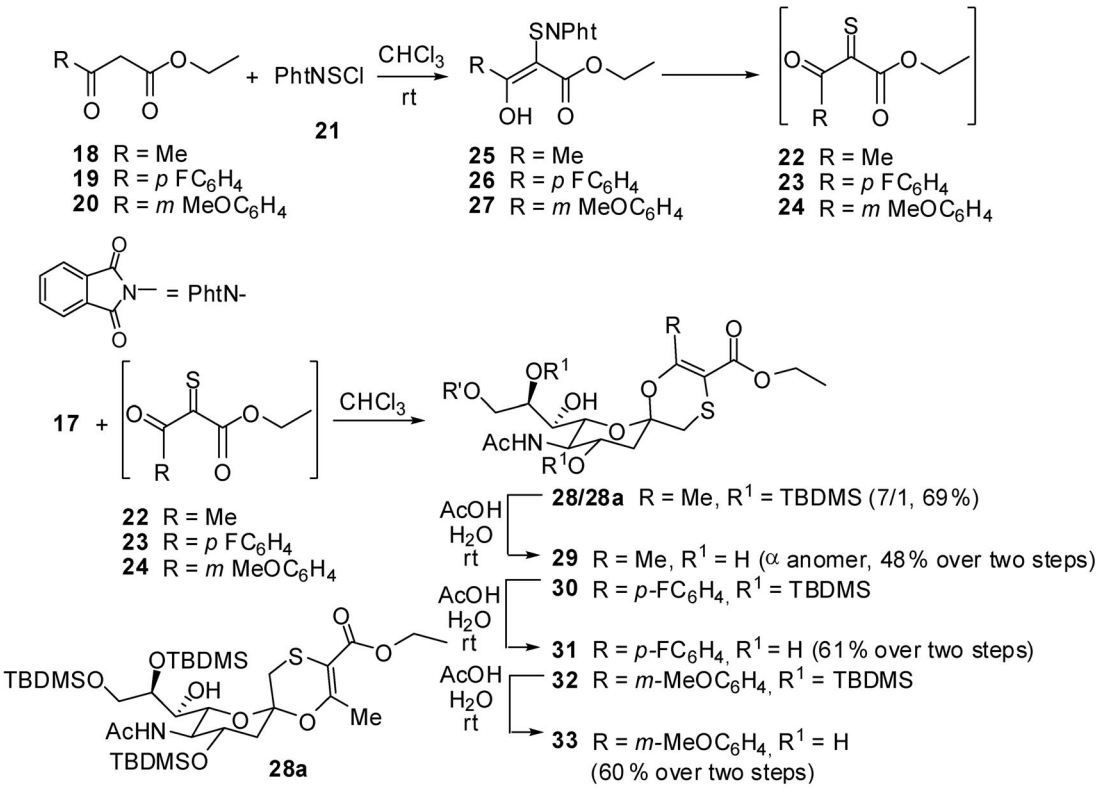

Scheme 3 Synthesis of cycloadducts **29**, **31**, and **33**.

The α,α'-dioxothiones **22–24** were formed under mild conditions from the phtalimido derivatives **25–27** and trapped in situ by the *exo*enitol **17** in an inverse electron-demand Diels–Alder reaction as reported in Scheme 3.

Synthesis of αNeu5Ac analogues

All the cycloadditions were totally chemo- and regioselective, in addition, cycloadducts **30** and **32** were obtained as single diasteroisomers. Conversely, the cycloadduct **28** was formed as a nonseparable mixture of diasteroisomers (**28** and **28a**) in a 7:1 ratio.

Capitalizing on results previously obtained [12], we hypothesized the formation of diasteroisomer **28**, which is the isomer with two anomeric effects, as the major one (see Scheme 3), which derives from the attachment of the diene to the upper face of the dienophile.

Silylethers were removed with AcOH/H_2O (4/1) from the mixture of **28** and **28a** and from cycloadducts **30** and **32** to obtain the corresponding sialyl spiroketals **29**, **31**, and **33** (Scheme 3). The ethyl ester **29**, isolated as pure α anomer, was hydrolyzed with lithium hydroxide in THF/H_2O as sol-

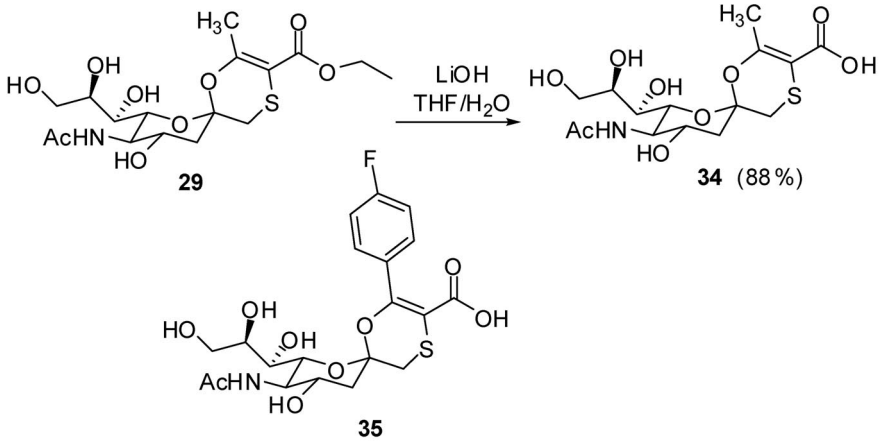

Scheme 4 Synthesis of sialyl spiroketals **34** and structure of **35**.

vent, to afford, in high yield, the completely deprotected spiroketal **34** as a diasteromerically pure compound (Scheme 4).

Molecular modeling

To obtain a putative binding mode of the newly synthesized compounds within the neuraminidase active site, we have undertaken docking calculation of compounds **34** and **35**. Their ethyl ester precursors were not considered in this study, since they are expected to be readily hydrolyzed by endogenous esterases in vivo. The crystallographic structure of the complex between sialic acid (α-Neu5Ac) and the influenza virus sialidase [14,15] was employed, in order to make a direct comparison between **34**, **35**, and the interactions of Neu5Ac with the active site residues (Fig. 3A). Two models for each compound were prepared as described in the experimental section, having the pyranose ring either in chair or boat configurations. Initially, redocking of Neu5Ac crystallographic structure was performed to assess the performance of the method employed. The top-ranked solutions belong to the highest populated cluster of bound conformations (78 %), and exhibited poses as low as 0.7–1.2 Å root-mean-square deviation with respect to the crystal structure. Therefore, bound conformations retained all intermolecular interaction with the neuraminidase active site residues (Fig. 3A), displaying only minimal differences at the glycerol moiety. The estimated mean free energy of binding for Neu5Ac was –5.8 Kcal/mol, corresponding to an inhibition constant of ~55 μM.

Analysis of the docking results obtained for compounds **34** and **35** revealed a high number of distinct conformational clusters, many of which adopted a completely different binding mode in comparison with Neu5Ac. This was the case for the majority of the predicted binding poses of both **34** and **35** with pyranose in the chair configuration, which resulted in an almost inverted binding mode of the pyranose ring with respect to Neu5Ac (i.e., the C5-acetamido group facing towards the three arginine residues 118, 292, and 371, Fig. 3A). As a consequence, most of the hydrogen-bonding interactions displayed by Neu5Ac and the active site residues of neuraminidase are lost. On the other hand, docking of **34** and **35** in the same boat configuration as that of the bound Neu5Ac exhibited two conformational clusters that approximate the binding mode of Neu5Ac. For compound **34**, the highest energy conformation of the top ranked cluster (15 %) with a mean free energy of binding of –5.0 Kcal/mol is shown in Fig. 3B. In this binding mode, the carboxylate group is slightly shifted with respect to that of sialic acid (<1 Å), thus maintaining the hydrogen-bonding network with Arg118, Arg292, and Arg371. However, for the proper accommodation of the oxathiine moiety inside the active site, the pyranose ring of **34** is rotated by ~45° and shifted towards residue Ile222 by ~3 Å, which results in loss of the

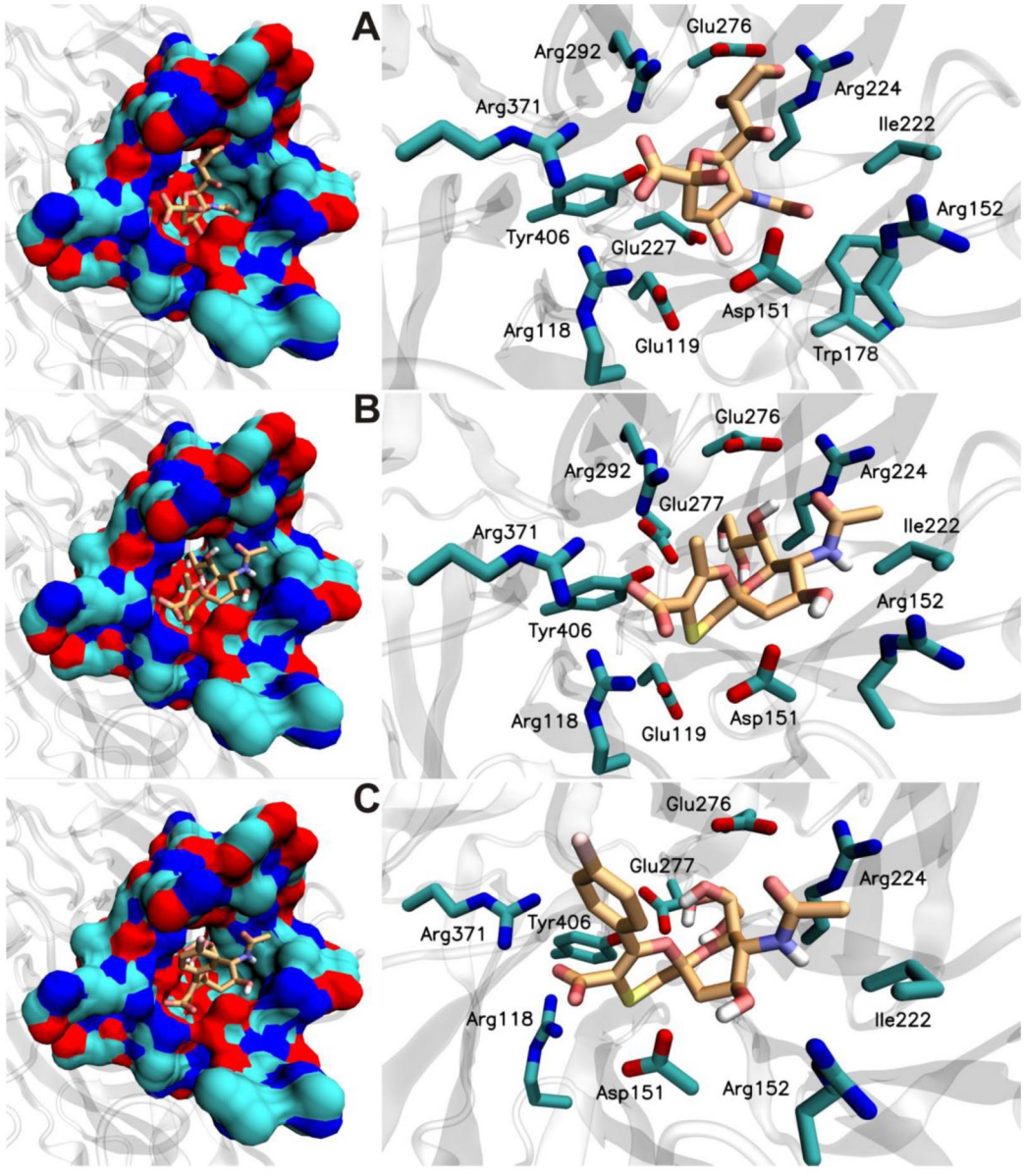

Fig. 3 (A) Crystallographic structure of α-Neu5Ac complex with influenza virus sialidase from PDB ID 2BAT with the active site residues represented as surface (left) and sticks (right). (B) and (C) illustrate the predicted conformations of **34** and **35**, respectively, and the interacting active site residues of sialidase. Protein side-chain atoms are labelled, and the ligands are colored in bright gray.

hydrophobic contacts with Trp178. Moreover, although the water-mediated interaction of Neu5Ac with Glu227 is possibly lost, the glycerol group of **34** is able to interact with Glu277 via a hydrogen bond. Overall, compound **34** is predicted to interact with most of the residues displayed by Neu5Ac–sialidase complex, albeit with a lower affinity that is mainly due to a loss of ~1.4 Kcal/mol in the electrostatic energy term.

As for compound **34**, the p-fluorophenyl substituent gives rise to a larger shift of the oxathiine ring towards Arg118, thus losing contact with Arg292 (Fig. 3C). In this binding mode, the p-fluorophenyl group does not display contacts with any protein residue. In addition, the interaction between C4-OH of **35** and Glu119 is not present, as well as Glu276 exhibits only van den Waals contacts with the glycerol side-chain. For these reasons, compound **35** is predicted to bind sialidase with an even lower affinity (mean free energy of binding of –4.1 Kcal/mol). At this point, it should be noted that the differences between the calculated binding free energies for compounds **34**, **35**, and Neu5Ac is indicative only, as it falls within the standard error of about 2–3 Kcal/mol reported for AutoDock4 [16].

Conclusively, the oxathiine ring of the spiroketal compounds might displace the pyranose ring from the crystallographic position displayed by sialic acid and its derivatives [14], though proper functionalization of the spiroketal scaffold could compensate for the interaction with key amino acid residues of neuraminidase. Considering also the plasticity of sialidases, as exemplified in the development of zanamivir and oseltamivir [14], a possible reorganization of their active site might result in tighter binding of the spiroketal scaffolds than predicted. In addition, reduction of their polarity with respect to Neu5Ac (calculated partition coefficients of **34** ClogP = –3.0, **35** ClogP = –1.5, and Neu5Ac ClogP = –3.6 [17]) might provide inhibitors with improved bioavailability. Taken together, the new spiroketal scaffolds could represent a novel class of sialidase inhibitors, and their biological investigation is underway.

EXPERIMENTAL

Materials and measurements

All solvents were of reagent grade quality and purchased commercially. All starting materials were purchased commercially and used without further purification. All NMR spectra were recorded on Varian instruments (200 or 400 MHz). The NMR spectra were referenced to solvent. Mass spectra were recorded on an LCQ-FLEET ion trap Thermo Fischer. ESI-MS analysis was performed both in positive or negative ion mode. Optical rotation measurements were carried out with a Jasco DIP-370 polarimeter.

Computational methods

The crystallographic structure of the complex between influenza virus neuraminidase and sialic acid (Neu5Ac) resolved at 2.0 Å was retrieved from the Protein Data Bank with accession code: 2BAT [15]. The ligands and water molecules were extracted from the protein structure, and all docking files were prepared with AutoDockTools 1.5 [18]. Polar hydrogen atoms and Gasteiger charges were added for both protein and ligand atoms. The initial models of compounds **34** and **35** were obtained using the programs OMEGA 2.4 [19] and VIDA 4.1 [20]. In particular, OMEGA was used to obtain low-energy conformers of **34** and **35** with the pyranose ring in the chair configuration. In addition, the crystallographic coordinates of sialic acid was used as template in VIDA, so as to obtain the structures in the boat conformation. Docking calculations were performed with AutoDock 4.2 [16], employing the Lamarckian genetic algorithm with the default parameters from AutoDock3 [21]. The search space was within a grid box centered at Neu5Ac with dimensions defined by 61 × 51 × 41 points of 0.375 Å spacing. For each calculation, 100 docking rounds were performed with a maximum of 25 million energy evaluations, and the resulting conformations were clustered using a tolerance of 2.0 Å. Protein–ligand interactions were visually examined using VMD 1.9 [22], which was also used for the preparation of Fig. 3. The calculation plugins of Marvin 5.10 [17] were used for the prediction of octanol–water partition coefficients ClogP using the weighted method with the default parameters. All calculations were performed using a Dual Xeon workstation running the Linux x86_64 kernel version 2.6.32-279.

SUPPORTING INFORMATION

Experimental details and data for new compounds associated with this article are available online (http://dx.doi.org/10.1351/PAC-CON-12-11-08).

ACKNOWLEDGMENT

The authors thank Ente Cassa di Risparmio di Firenze (ECR) for financial support.

REFERENCES

1. (a) R. Schauer. *Glycoconjugate J.* **17**, 485 (2000); (b) H.-J. Gabius, S. André, J. Jimenez-Barbero, A. Romero, D. Solìs. *Trends Biochem. Sci.* **36**, 298 (2011).
2. E. R. Vimr, K. A. Kalivoda, E. L. Deszo, S. M. Steenbergen. *Microbiol. Mol. Biol. Rev.* **68**, 132 (2004).
3. R. Wagner, M. Matrosovich, H. D. Klenk. *Rev. Med. Virol.* **12**, 159 (2002).
4. P. M. Colman, J. N. Varghese, W. G. Laver. *Nature* **303**, 41 (1983).
5. J. N. Varghese, W. G. Laver, P. M. Colman. *Nature* **303**, 35 (1983).
6. Q. M. Le, M. M. Kiso, K. K. Someya, Y. T. Sakai, T. H. Nguyen, K. H. L. Nguyen, D. N. Pham, H. H. Ngyen, S. Yamada, Y. Muramoto, T. Horimoto, A. Takada, H. Goto, T. Suzuki, Y. Suzuki, Y. Kawaoka. *Nature* **437**, 1108 (2005).
7. M. G. Ison. *Curr. Opin. Virol.* **1**, 563 (2011).
8. P. W. Smith, S. L. Sollis, P. D. Howes, P. C. Cherry, I. D. Starkey, K. N. Cobley, H. Weston, J. Scicinski, A. Merritt, A. Whittington, P. Wyatt, N. Taylor, D. Green, R. Bethell, S. Madar, R. -J. Fenton, P. J. Morley, T. Pateman, A. Beresford. *J. Med. Chem.* **41**, 787 (2012).
9. B. Bhatt, R. J. Thomson, M. von Itzstein. *Bioorg. Med. Chem. Lett.* **22**, 7623 (2012).
10. S. Rudrawar, J. C. Dyason, M.-A. Rameix-Welti, F. J. Rose, P. S. Kerry, R. J. M. Russel, S. van der Welf, R. J. Thomson, N. Naffakh, M. von Itzstein. *Nat. Commun.* **113**, 1 (2010).
11. (a) Y. Du, R. J. Linhardt, I. R. Vlahov. *Tetrahedron* **54**, 9913 (1998); (b) T. V. RajanBabu, G. S. Reddy. *J. Org. Chem.* **51**, 5458 (1986).
12. G. Capozzi, C. Nativi, A. Bartolozzi, C. Falciani, S. Menichetti, A. Paolacci. *J. Org. Chem.* **64**, 6490 (1999).
13. (a) A. Bartolozzi, S. Pacciani, C. Benvenuti, M. Cacciarini, F. Liguori, S. Menichetti, C. Nativi. *J. Org. Chem.* **68**, 8529 (2003); (b) G. Capozzi, R. W. Franck, M. Mattioli, S. Menichetti, C. Nativi, G. Valle. *J. Org. Chem.* **60**, 6416 (1995).
14. M. von Itzstein. *Nat. Rev. Drug Discovery* **6**, 967 (2007).
15. J. N. Varghese, J. L. Mckimm-Breschkin, J. B. Caldwell, A. A. Kortt, P. M. Colman. *Proteins* **14**, 327 (1992).
16. G. M. Morris, R. Huey, W. Lindstrom, M. F. Sanner, R. K. Belew, D. S. Goodsell, A. J. Olson. *J. Comput. Chem.* **16**, 2785 (2009).
17. ChemAxon, http://www.chemaxon.com
18. M. F. Sanner. *J. Mol. Graphics Mod.* **17**, 57 (1999).
19. OpenEye Scientific Software, http://www.eyesopen.com/vida
20. P. C. D. Hawkins, A. G. Skillman, G. L. Warren, B. A. Ellingson, M. T. Stahl. *J. Chem. Inf. Model.* **50**, 572 (2010).
21. G. Morris, D. Goodsell, R. Halliday, R. Huey, W. Hart, R. Belew, A. J. Olson. *J. Comput. Chem.* **19**, 1639 (1998).
22. W. Humphrey, A. Dalke, K. Schulten. *J. Mol. Graphics* **14**, 33 (1996).

